1 July 2002

Optics Communications 208 (2002) 51–60

OPTICS COMMUNICATIONS

www.elsevier.com/locate/optcom

A pyramid wavefront sensor with no dynamic modulation

Roberto Ragazzoni[a,b], Emiliano Diolaiti[c], Elise Vernet[a,*,1]

[a] *INAF-Astrophysical Observatory of Arcetri, Largo E. Fermi 5, I-50125 Firenze, Florence, Italy*
[b] *Max-Planck-Institut für Astronomie, Königstuhl 17, D-69117 Heidelberg, Germany*
[c] *Department of Astronomy, Vicolo dell'Osservatorio 2, I-35122 Padova, Italy*

Received 1 February 2002; received in revised form 10 May 2002; accepted 22 May 2002

Abstract

The pyramid wavefront sensor has been introduced in the field of astronomical adaptive optics a few years ago. An important issue characterizing this wavefront sensor is how to reach high dynamical range, a task realized so far by either vibrating the pyramid or oscillating a tip-tilt mirror in a plane conjugated to the exit pupil of the telescope. A new method is proposed here to achieve the same result, without any moving part: the new approach is based on a light diffusing plate placed in an intermediate pupil plane. Some practical implementations of this concept are presented and the relevance to multi-conjugate adaptive optics is discussed.

Keywords: Adaptive Optics; Pyramid wavefront sensor; Diffusing plate

1. Introduction

The Pyramid WaveFront Sensor (PS) (Ragazzoni [1]) is based on an oscillating pyramidic optical component, placed at the focal plane of the aberrated optical system e.g., a telescope in astronomical adaptive optics (Ragazzoni et al. [2], [3]). The pyramid splits the light in four beams, which are imaged by a relay optics onto an observation plane, producing four images of the pupil. These four intensity patterns, suitably combined, provide information on the derivatives of the aberrated wavefront. In the absence of oscillation, the PS is fully equivalent to a Foucault test [4] and, in the geometrical optics approximation, it allows to retrieve only the sign of the wavefront derivatives. In fact, a given ray coming from the point P on the exit pupil hits a face of the pyramid and only the pupil image corresponding to this face is illuminated at the point P′ conjugated to P (see Fig. 1). When a modulation is applied, instead, the ray spends a fraction of the time on every face of the pyramid, so that all the four pupil images are more or less illuminated in the point P′ conjugated to P, giving a useful signal to compute the wavefront derivatives.

The modulation radius r of the pyramid determines the sensitivity and the dynamic range of the PS (Fig. 2). A small modulation amplitude (Fig.

* Corresponding author. Tel.: +390552752273; fax: +39055220039.
E-mail address: elise@arcetri.astro.it (E. Vernet).

[1] This work has been partially funded by the European Research and Training Network *Adaptive Optics for Extremely Large Telescopes* with Contract HPRN-CT-2000-00147.

0030-4018/02/$ - see front matter
PII: S0030-4018(02)01580-8

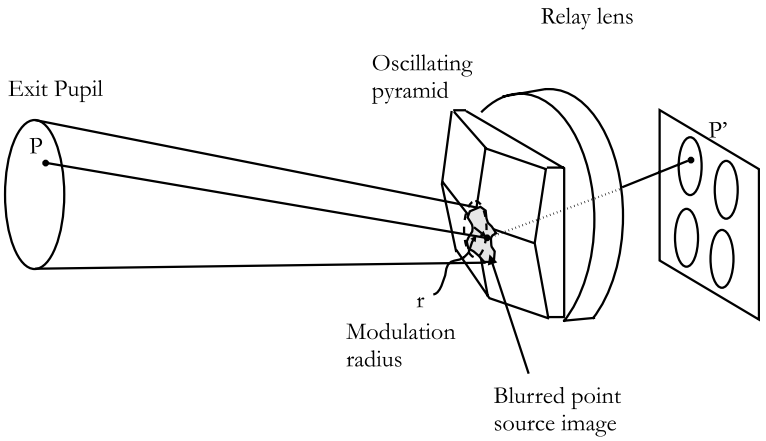

Fig. 1. System layout. A given ray coming from the point P hits a face of the pyramid and illuminates the corresponding pupil image in P′, the point conjugated to P. Due to the pyramid modulation of radius r, the ray spends a fraction of the time on every face of the pyramid, so that all the four pupil images are more or less illuminated in P′.

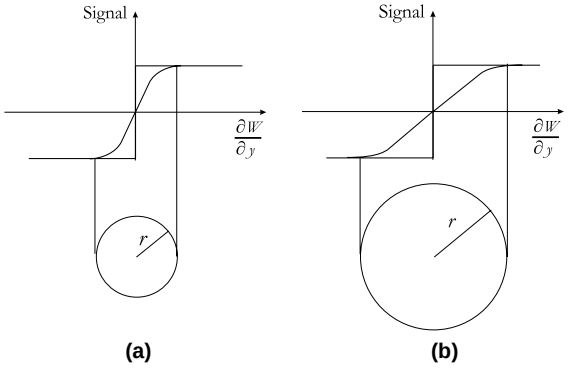

Fig. 2. Pyramid wavefront sensor signal as a function of the wavefront aberrations for different modulation amplitudes.

2(a)) produces a large signal even with small wavefront aberrations, whereas a large modulation r (Fig. 2(b)) makes the response curve less steep and allows the measurement of larger aberrations. In the early stages of a closed loop operation of an Adaptive Optics (AO) system, a large modulation amplitude is usually well suited as the correction is only partial and large aberrations are present. When the correction improves and the loop is closed, the aberrations decrease, the required dynamic range is smaller and a lower modulation can be used, leading to a better sensitivity. Thanks to this feature the PS yields better performance than a Shack–Hartmann (SH) wavefront sensor, as it has been shown by Ragazzoni and Farinato [5] and by Esposito and Riccardi [6]. The most remarkable consequence for astronomical AO systems is the gain in limiting magnitude of the reference source.

The PS modulation may be accomplished by physically vibrating the pyramid (Ragazzoni [1]) or by oscillating a tip-tilt mirror conjugated to the exit pupil of the system (Riccardi [7]). The former method has been used on AdOpt@TNG, the adaptive optics module at the Telescopio Nazionale Galileo (Ragazzoni et al. [8]). The major drawback of these solutions is the presence of moving parts. In this paper we introduce a *static* modulation method, fully equivalent to the dynamic one, without using any moving component. The new concept is based on a light diffusing element placed in an intermediate pupil plane, which causes a blur of the spot on the pyramid pin, in a similar way to the dynamic modulation.

In the following, we derive a relationship between the blur introduced by this device and the dynamic modulation amplitude and we discuss some practical implementations of this new idea. Finally we discuss the relevance of this new concept to multi-conjugate adaptive optics (Beckers [9]; Ellerbroek [10]; Johnston and Welsh [11]; Ellerbroek and Rigaut [12]; Ragazzoni et al. [13]; Tokovinin et al. [14] for examples) and in particular

to the layer-oriented approach (Ragazzoni [15]; Ragazzoni et al. [16]; Diolaiti et al. [17]; Ragazzoni et al. [18]), for which the static modulation method presented here might lead to interesting advantages both in terms of opto-mechanical simplicity and optimal weighting of the reference signals.

2. The static method

The effect of the tip-tilt modulation is a blur of the spot on the pyramid pin. The same result can be achieved with a light diffusing element placed in an intermediate image of the pupil. A possible optical layout of the concept is shown in Fig. 3.

A collimating lens (L_1) is placed behind the focal plane of a telescope of diameter D. For simplicity we assume a telecentric system, even though this is not a necessary condition. The lens produces an intermediate image of the pupil of size d in the focal plane of L_1; we just mention here that in case of a non-telecentric beam, the pupil image is produced at a different distance from L_1. A light diffusing element is placed in the intermediate pupil and spreads each incident ray with a given probability distribution within a cone of semi-aperture α; the axis of the cone coincides with the initial direction of the ray. Even though the diffusion is assumed to be random here, this is not a strictly necessary condition and some other approaches are described in Section 4. Before going further, we want to emphasize that the phase information contained in the spot is preserved to some extent: the axis of propagation of the beam remains identical after the diffusing plate, inducing a conservation of relative phase information.

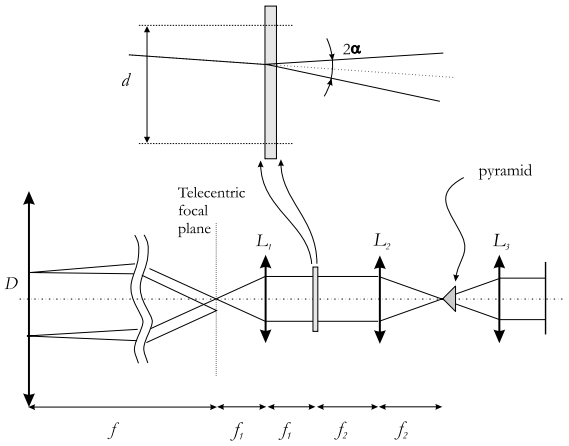

Fig. 3. Illustration of the concept. A diffusing element placed in the intermediate pupil between lenses L_1 and L_2 produces a blur of the spot on the pyramid pin. A further lens (L_3) re-images the four beams (not shown here) produced by the pyramid, forming four images of the pupil on the observation plane.

Such a phase conservation can be stated in a more detailed form in the following way: let us assume that the wavefront deformation introduced by the diffuser in a single sub-aperture sampled by the WFS is denoted by $\tilde{W}(x,y)$. The requirement for phase conservation can be expressed as

$$\int_{\text{subaperture}} I_{\text{N}}(x,y)\frac{\partial\tilde{W}(x,y)}{\partial x} \ll \frac{\lambda}{D} \tag{1}$$

(and the symmetric in y) where I_{N} is the illumination within the sub-aperture, normalized to unit integral. In the case of sub-apertures well within the boundaries of the pupil this does not impose any particular requirement on the so-called diffusing plate. However special attention should be given to the sub-apertures situated at the edges. Actually, the condition

$$\left\langle \frac{\partial\tilde{W}}{\partial x} \right\rangle \ll \frac{\lambda}{D} \tag{2}$$

and its symmetric in y fullfil Eq. (1) only in the case of uniform illumination across the sub-aperture. A function for $\tilde{W}(x,y)$ with a much higher spatial frequency than the inverse of the sampling sub-aperture will be better suited at the edges but it will produce a larger amount of scattered light. On this basis one should find a compromise and choose the best spatial frequency for such a diffusing plate. In the following we limit ourselves to outline the theory and to provide an example of possible diffusing plates.

A second lens (L_2) focuses the beam onto the pyramid pin: the spot is blurred because of the random spreading of the rays due to the diffusing plate. This blur is equivalent to a dynamic modulation of the pyramid. The pyramid splits the beam into four parts, imaged by lens L_3 onto the observation plane, forming four images of the

pupil: the recorded intensity pattern is then used to compute the wavefront aberrations. It should be stressed that the observation plane is conjugated with the intermediate pupil, i.e., with the diffusing plate, therefore no additional blur occurs on the four pupil images and the wavefront information is not degraded.

The spreading angle α is a free parameter characterizing the diffusing element: it can be tuned in order to have a pre-fixed blur at the focal plane where the pyramid is placed. For instance it may be desirable to have a spot radius r equal to that produced by the dynamic modulation. It is straightforward to see from Fig. 4 that the spreading angle α and the linear spot size r on the focal plane are linked by the relationship $r = \alpha f_1$ where f_1 is the focal length of lens L_1. In the small angle approximation, the linear size r corresponds to an angle $\beta = r/f$ seen from the system aperture, where f is the focal length of the system itself. Combining the last two equations and considering that $f/f_1 = D/d$, (d is the size of the intermediate image of the pupil) one obtains

$$\alpha = \beta \frac{D}{d}. \tag{3}$$

A suitable choice for the angular size of the spot is a few times the telescope diffraction limit, i.e., $\beta = N\lambda/D$, corresponding to a diffusing angle

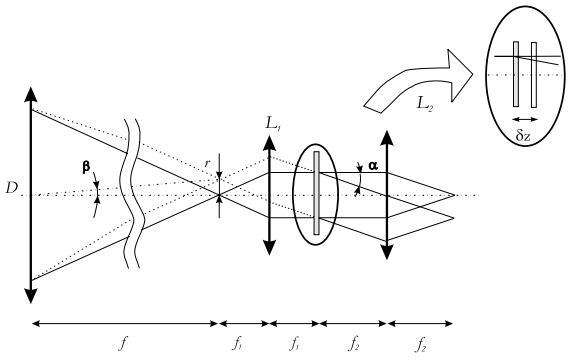

Fig. 4. Relationship between diffusing angle and spot size. The spot size in the focal plane after L_2 is f_2/f_1 times larger than in the focal plane before L_1. The quantity δz represents the positioning accuracy of the plate.We show in the text that a displacement of the diffusing plate of δz induces a blur of the intermediate pupil.

$$\alpha = N \frac{\lambda}{d}. \tag{4}$$

As already stated, the blur introduced by the diffusing plate does not affect the image on the detector plane. This is true provided that the plate is accurately positioned in the plane of the intermediate pupil. A displacement δz (see Fig. 4) along the optical axis produces a blur of the intermediate pupil over a spatial scale $\alpha\delta z$. The effect is negligible if this length is much smaller than the typical scale of interest, on which the wavefront aberrations are measured, usually represented by the Fried parameter r_0. Considering that each length on the telescope aperture scales as d/D on the intermediate pupil and recalling Eq. (4), we conclude that the positioning error is negligible if

$$\delta z \ll \frac{r_0 d^2}{DN\lambda}. \tag{5}$$

For $D = 8$ m, $\lambda = 5 \times 10^{-7}$ m, $r_0 = 0.1$ m, $d = 10^{-3}$ m, we obtain $\delta z \ll 0.025/N$ m. With $N = 3$ (Esposito and Riccardi [6]), δz has to be smaller than $\approx$0.8 mm, an easily achievable precision.

3. Comparison with dynamic modulation

The diffusing angle α has to be adjusted so that the blur effect is equivalent to that obtained by a dynamic modulation of given amplitude r. A possible figure of merit, adopted in the previous section, is to impose the same spot size. In closed-loop, however, the equivalence may be imposed by requiring that the two methods have the same gain, represented by the derivative of the response curve sketched in Fig. 2, evaluated in the neighborhood of the origin.

In order to make a quantitative comparison, we consider the geometry shown in Fig. 5, where a ray affected by an aberration in the y direction hits the pyramid surface at the point of coordinates $(0, y_0)$. In the static method we can associate to the incidence point an intensity distribution which is strictly related to the diffusing probability density in case of random

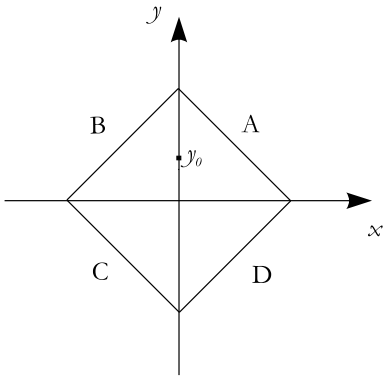

Fig. 5. Coordinates on the pyramid wavefront sensor.

scattering. We assume for simplicity a gaussian distribution

$$g(x,y) = \frac{1}{2\pi\sigma^2} e^{(-(x^2+(y-y_0)^2)/2\sigma^2)} \tag{6}$$

whose standard deviation σ is proportional to the diffusion angle α of the plate.

The pyramid divides the light in four parts giving then four exit pupils. The signal of the PS is defined by

$$S = \frac{I^+ - I^-}{I^+ + I^-}, \tag{7}$$

where I^+ and I^- are, respectively, $I_A + I_B$ and $I_C + I_D$ when considering the aberrations on the y axis direction (A, B, C ,D are defined in Fig. 5). The intensity I^+ is obtained by integrating the distribution $g(x,y)$ on the upper part of the pyramid:

$$\begin{aligned} I^+ &= \int_{-\infty}^{\infty}\int_{0}^{\infty} g(x,y)\,dx\,dy \\ &= \frac{1}{\sqrt{2\pi}\sigma}\int_{0}^{\infty} e^{(-(y-y_0)^2/2\sigma^2)}\,dy. \end{aligned} \tag{8}$$

The intensity I^- coming from the lower part of the pyramid is obtained equivalently:

$$I^- = \frac{1}{\sqrt{2\pi}\sigma}\int_{-\infty}^{0} e^{(-(y-y_0)^2/2\sigma^2)}\,dy. \tag{9}$$

We feed Eqs. (8) and (9) into Eq. (7); after some change of integration variable and re-arrangement of the various integrals, we finally obtain

$$S = \sqrt{\frac{2}{\pi}}\frac{1}{\sigma}\int_{0}^{y_0} e^{-y^2/2\sigma^2}\,dy. \tag{10}$$

The quantity of interest is the derivative of the signal S to the aberration y_0, given by

$$\frac{\partial S}{\partial y_0} = \sqrt{\frac{2}{\pi}}\frac{1}{\sigma} e^{-y_0^2/2\sigma^2}. \tag{11}$$

In the case of a dynamic modulation, the signal depends on the modulation shape. As already demonstrated in previous papers on the PS (Ragazzoni [1], Riccardi et al. [19]), with a circular modulation of radius r it can be shown that

$$I^+ \propto \pi + 2\sin^{-1}\left(\frac{y_0}{r}\right), \tag{12}$$

$$I^- \propto \pi - 2\sin^{-1}\left(\frac{y_0}{r}\right). \tag{13}$$

It should be noticed that the modulation radius r in the last two equations is measured on the focal plane after lens L_2 (see Fig. 3) and therefore it is a factor f_2/f_1 larger than on the telescope focal plane, where the PS is usually placed in the standard approach. The signal can be deduced replacing Eqs. (12) and (13) in Eq. (7):

$$S = \frac{2}{\pi}\sin^{-1}\left(\frac{y_0}{r}\right). \tag{14}$$

The derivative of the signal to y_0 is

$$\frac{\partial S}{\partial y_0} = \frac{2}{\pi r}\frac{1}{\sqrt{1-\left(\frac{y_0}{r}\right)^2}}. \tag{15}$$

Equalizing Eqs. (11) and (15) for $y_0 = 0$ we obtain

$$\sigma = r\sqrt{\frac{\pi}{2}}. \tag{16}$$

The modulation radius is directly proportional to the standard deviation σ of the scattering probability density. Replacing the Full Width Half Maximum (FWHM) to the standard deviation, we obtain

$$\mathrm{FWHM} = 2\sqrt{\pi\ln 2}r \simeq 2.95 \times r. \tag{17}$$

According to the geometrical relations introduced in the previous section, this linear size on the focal plane corresponds to a certain diffusing angle on the plate, depending on the focal length f_2 of the lens.

4. Possible implementations

A very simple diffusing element is represented by a glass plate with *rough* surface. This device produces a random spreading of the incident rays, with a gaussian probability distribution. The surface irregularities must occur at spatial scales smaller than a typical length related to the spreading angle α, so that the surface can be considered perfectly flat over larger scales. An upper limit for this spatial scale is represented by the pupil sampling step s, scaled by a factor d/D over the pupil image; this condition ensures that no blur occurs on scales larger than the typical length over which the wavefront aberrations are measured. In astronomical adaptive optics, the sampling step is usually matched to the Fried parameter r_0 (Fried [20]), which represents the coherence length of the atmospheric turbulence. A spatial power spectrum which might describe such a surface roughness is shown in Fig. 6.

A second possibility is an array of micro-lenses, similar those used in SH wavefront sensors. In this case the light diffusion is not random: the effect of each lenslet is to focus a portion of the beam in front of lens L_2 (Fig. 3), so that the overall beam is spread over the desired angular range. The diffusing angle is $\alpha = 1/(2F)$, where F is the focal ratio of a lenslet. The lenslet pitch must be smaller than the equivalent sampling size sd/D.

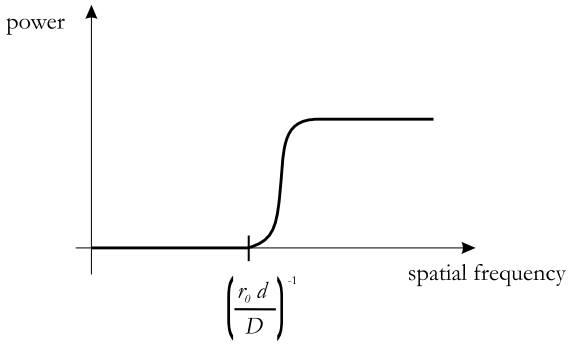

Fig. 6. Surface roughness power spectrum of the diffusing glass plate. The minimum spatial frequency for the surface irregularities is in the particular case the inverse of the equivalent r_0 size.

A further implementation is based on a phase grating, which produces an array of spots, as in Fig. 7. The phase perturbations must occur at spatial scales smaller than the sampling step size and this imposes some constraints on the angular separation of the diffraction orders. The resulting light distribution does not appear as a continuous one even after an optimization of the curve by adjusting the orientation of the grating.

These problems might be overcome using holographic diffusers (Wadle et al. [21], Wenyon and Ralli [22], Wadle and Lakes [23]), which allow a more accurate shaping of the intensity distribution on the focal plane. An holographic diffuser which diffracts the light with the desired spatial distribution can be obtained by selectively recording the diffused wave in certain directions. Gu et al. [24] pointed out that usually holographic diffusers are monochromatics. They investigated different kinds of diffuser materials and showed that by selecting the diffuser medium one can create polychromatic diffuser of good quality.

5. Relevance to multi-reference wavefront sensing

In layer-oriented multi-conjugate adaptive optics (see for instance Ragazzoni et al. [16]), each reference star is coupled to a pyramid and the pupil images corresponding to different stars are optically co-added by a re-imaging lens (see Fig. 8).

The diffusing plate concept proposed in this paper may be generalized to the multi-reference case, according to the layout sketched in Fig. 9, where a different diffusing plate is associated with each star. An alternative approach would be to use a single diffusing element, placed in a pupil plane before the pyramids, even though this might translate into additional constraints on the opto-mechanical design of the whole system. Furthermore the solution presented in Fig. 9 offers an additional degree of freedom, represented by the spreading angle of each plate, which might be adjusted in order to achieve an optimal weighting of the reference signals.

The concept of optimality mentioned here is closely related to the uniformity of correction

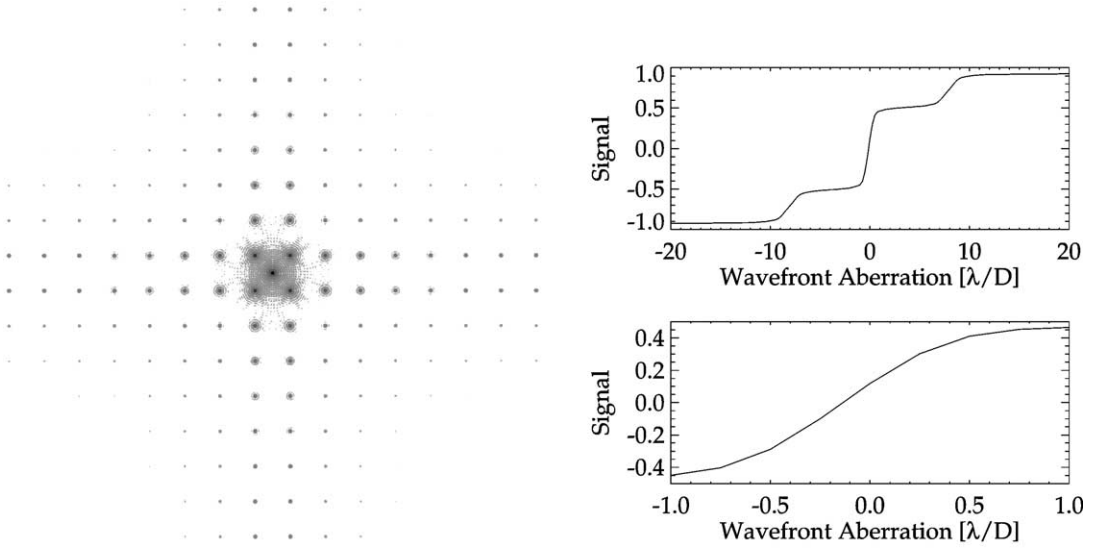

Fig. 7. Left: diffraction pattern produced by a phase grating with square elements, illuminated by a beam of circular section. Right: response curve for large (top) and small (bottom) wavefront aberrations.

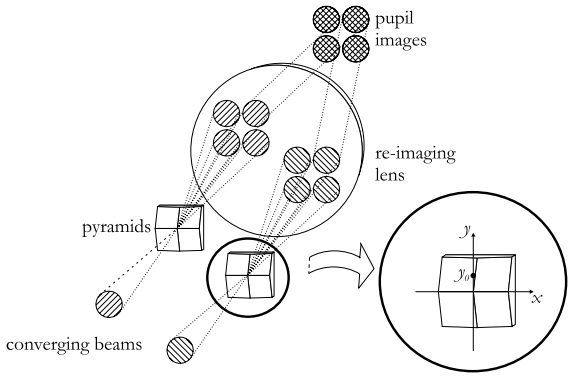

Fig. 8. The pyramids in the focal plane of the telescope, one for each reference star, split the light into four beams. A re-imaging lens combines the light of the various stars forming four pupil images on the observation plane. The recorded intensity at every point of this plane is the sum of the single star contributions.

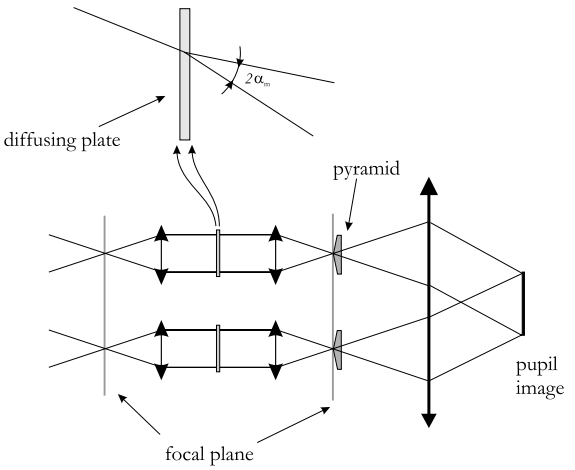

Fig. 9. A generalization of the opto-mechanical layout of Fig. 3, extended to the case of multiple references.

across the field of view. Fig. 10 illustrates how the footprints of some reference stars might be displaced on a high altitude layer: this uneven spatial distribution translates into a non-uniform photon density and therefore into a spatially varying measurement error on the wavefront. Since the wavefront variance is closely related to the achievable Strehl ratio, it is clear that the net effect is a non-uniform correction across the field of view. Actually the photon density uniformity is determined by two factors: the spatial distribution of the stars and their relative brightness.

A general discussion of the concept of optimal weighting is beyond the scope of this work and we consider here some limiting cases. An interesting example is the situation in which the reference

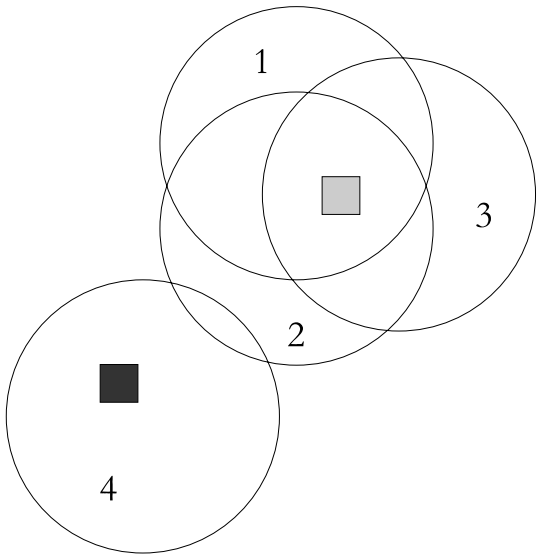

Fig. 10. The footprints of the reference stars do not overlap on the high altitude atmospheric layers, therefore the photon density is not homogeneous and the wavefront measurement error changes across the field.

stars have different brightness but their spatial distribution is uniform. In this case we consider first the signal corresponding to a wavefront aberration $\partial W_m/\partial y$ experienced by the mth star. According to Eq. (10), it is given by

$$S_m = \sqrt{\frac{2}{\pi}}\frac{1}{\sigma_m}\int_0^{y_0} \mathrm{e}^{-y^2/2\sigma_m^2}\,\mathrm{d}y, \tag{18}$$

where y_0 is the transverse ray aberration on the focal plane. More general aberrations, involving the orthogonal direction x, are treated in a similar way, but are not considered here for simplicity. We recall again that the standard deviation σ_m defining the intensity distribution on the pin of a given pyramid is proportional to the diffusion angle α_m on the corresponding diffusing plate. In closed loop operation, the residual aberrations y_0 may be considered smaller than the standard deviation σ_m of the mth star, allowing to simplify Eq. (18) as

$$S_m \approx \sqrt{\frac{2}{\pi}} f \frac{1}{\sigma_m}\frac{\partial W_m}{\partial y}, \tag{19}$$

showing that the signal S_m of the mth star is proportional to the wavefront aberration. This signal is obtained by linear combinations of the recorded intensity values, according to the expression

$$S_m = \frac{I_m^+ - I_m^-}{I_m} \tag{20}$$

where I_m^+ and I_m^- are the intensities integrated on the semi-planes corresponding to positive and negative y values and I_m is the total intensity of the star. In the multi-reference layer-oriented approach, the light of the stars is optically co-added on the detector, so that the intensity in each point is the sum of the contributions of each single star (Fig. 8). Eq. (20) can be generalized as

$$S = \frac{I^+ - I^-}{I}, \tag{21}$$

where $I^+ = I_1^+ + I_2^+ + \cdots + I_M^+$, $I^- = I_1^- + I_2^- + \cdots + I_M^-$ and I is the total intensity of all the reference stars. Re-arranging Eq. (21), it is straightforward to obtain

$$S = \frac{(I_1^+ - I_1^-) + \cdots + (I_M^+ - I_M^-)}{\sum_m I_m} \propto \sum_m I_m S_m, \tag{22}$$

showing that the overall signal is the average of the single star signals weighted by the corresponding intensity. Of course the latter relation holds wherever all the star footprints overlap at the considered detector location. Replacing Eq. (19) in Eq. (22), one obtains the signal as a function of the wavefront aberrations experienced by the single stars:

$$S \propto \sum_m \frac{I_m}{\sigma_m}\frac{\partial W_m}{\partial y}. \tag{23}$$

Considering that the signal S is proportional to the estimated wavefront derivative $\partial W/\partial y$, the last expression can be recast to the form

$$\frac{\partial W}{\partial y} \propto \sum_m \frac{I_m}{\sigma_m}\frac{\partial W_m}{\partial y}, \tag{24}$$

which is a generalization of the relationship shown in Ragazzoni et al. [16]. Using for each star a proper diffusing plate such that

$$\sigma_m = \sigma\frac{I_m}{\sum_m I_m} \tag{25}$$

the contributions of the stars are averaged regardless the corresponding intensity I_m. The

proportionality constant σ may be fixed for a given state of the loop: a large value of this parameter, for instance, is well suited to the early phases, when the correction is poor, the aberrations are large and a high dynamic range is required. Apart from this factor, the diffusion coefficient of a given star is proportional to the relative intensity. In this way the linear combination of the single star wavefront derivatives is more sensitive to the faint references and the net effect is equivalent to a uniform photon density across the field of view (see also Fig. 11).

It should be stressed that decreasing the sensitivity of the PSs associated to the bright stars translates into a worsening of the signal-to-noise ratio (SNR). In some cases, when the brightness range spanned by the stars is not too large, it might be convenient to skip the optimization described before. It is also noticeable that whenever the intensity ratio between the brighter and dimmer reference stars is smaller than $I_{\max}/I_{\min} \leqslant D/r_0$, the PS still gives an improved SNR with respect to the SH one, although not as large as that given in Ragazzoni and Farinato [5] and in Esposito and Riccardi [6]. Of course in a realistic situation, the spatial distribution of the stars is not uniform as assumed above. Therefore the optimal weighting must take into account both the brightness of the stars and their relative distances. Stars within the same isoplanatic patch can be treated as a single source of equivalent brightness given by the sum of the various contributions, whereas the remaining stars have to be weighted accordingly to the inverse of their relative distance from the centroid of the stars asterism.

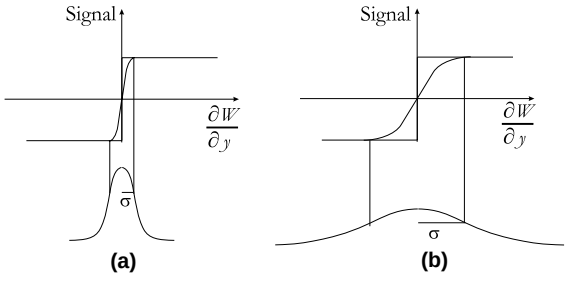

Fig. 11. The gain of the PS can be adjusted tuning the equivalent modulation σ. The same wavefront aberration gives a larger signal when the equivalent modulation is smaller.

6. Conclusions

The PS is a kind of quantitative two dimensional Foucault test which divides the incoming light in four exit pupils. In order to determine the wavefront derivatives, the light coming from each portion of the exit pupil has to be spread over all four pupil images. Up to now, such condition was realized by modulating the spot image. We have described here an equivalent static method, based on a very simple light diffusing element placed in an intermediate pupil plane, which accomplishes the required blur so that all the four pupil are enlightened. The great advantage of this solution is the absence of any moving part. With a quantitative comparison of the static and dynamic approach, we have determined the relationship between the modulation radius and the diffusion angle giving an equivalent response in closed loop.

The proposed solution, thanks to its opto-mechanical simplicity, fits naturally the framework of layer-oriented multi-conjugate adaptive optics (Ragazzoni et al. [25]). Using a diffusing plate for each reference star allows in principle to optimize the weighting of the reference signals and achieve a uniform photon density on the upper portion of the sensed turbulence, ensuring a more homogeneous correction across the field of view.

One of the advantages of the PS is the capability to change the gain curve when the loop is closed by reducing the modulation radius. In the static case the same result may be achieved using for instance a circular plate with different scattering angles on different portions of its surface; turning the plate on its axis would allow to change the gain curve in closed loop.

As a concluding remark, we just mention here that the modulation of the PS, either dynamic or static, might require some further revision. In fact an astronomical adaptive optics system is optimized to achieve best performance in a certain wavelength range, usually in the near infrared, while wavefront sensing is performed at a shorter wavelength, typically in the visible. The size of the pupil sampling sub-apertures for wavefront sensing is usually matched to the value of the Fried parameter r_0 at the longer wavelength, which is larger than the value of r_0 in the visible. All the

wavefront aberrations occurring at spatial scales smaller than the sub-aperture size are essentially uncorrected, leaving a residual blur of the spot at the wavefront sensing wavelength which might turn out to be substantially equivalent to the effect of the pyramid modulation, either dynamic or static. This point, although very interesting, is beyond the scope of this work and is left to further investigation.

Acknowledgements

Thanks are due to Jacopo Farinato and Enrico Marchetti for the useful discussions on the concept presented in this paper. This work has been partially funded by the European Research and Training Network *Adaptive Optics for Extremely Large Telescopes* with Contract HPRN-CT-2000-00147.

References

[1] R. Ragazzoni, J. Mod. Opt. 43 (1996) 289.
[2] R. Ragazzoni, A. Ghedina, A. Baruffolo, E. Marchetti, J. Farinato, T. Niero, G. Crimi, M. Ghigo, SPIE Proc. 4007 (2000) 423.
[3] R. Ragazzoni, A. Baruffolo, J. Farinato, A. Ghedina, E. Marchetti, S. Esposito, L. Fini, P. Ranfagni, F. Bortoletto, M. D'Alessandro, M. Ghigo, G. Crimi, SPIE proc. 4007 (2000) 57.
[4] L.M. Foucault, Ann. Obs. Imp. Paris 5 (1859) 197.
[5] R. Ragazzoni, J. Farinato, A&A 350 (1999) L23.
[6] S. Esposito, A. Riccardi, A&A 369 (2001) L9.
[7] A. Riccardi, Degree thesis, University of Firenze-Italy, 1996.
[8] R. Ragazzoni, A. Baruffolo, J. Farinato, A. Ghedina, S. Mallucci, E. Marchetti, T. Niero, SPIE Proc. 3353 (1998) 132.
[9] J.M. Beckers, in: ESO Conference on Very Large Telescopes and Their Instrumentation, 1988, p. 693.
[10] B.L. Ellerbroek, JOSAa 11 (1994) 783.
[11] D.C. Johnston, B.M. Welsh, JOSAa 11 (1994) 394.
[12] B.L. Ellerbroek, F. Rigaut, Nature 403 (2000) 25.
[13] R. Ragazzoni, E. Marchetti, G. Valente, Nature 403 (2000) 54.
[14] A. Tokovinin, M. Le Louarn, E. Viard, N. Hubin, R. Conan, A&A 378 (2001) 710.
[15] R. Ragazzoni, in: T. Andersen, A. Ardeberg, R. Gilmozzi (Eds.), ESO Proceedings of the Backaskog workshop on extremely large telescopes, 57, 1999, p. 175.
[16] R. Ragazzoni, J. Farinato, E. Marchetti, in: Wizinowich (Ed.), SPIE Proc., 4007, 2000, p. 1076.
[17] E. Diolaiti, R. Ragazzoni, M. Tordi, A&A 372 (2001) 710.
[18] R. Ragazzoni, S. Esposito, E. Vernet-Viard, A. Baruffolo, M. Carbillet, E. Diolaiti, R. Falomo, J. Farinato, E. Marchetti, M. Tordi, ESO Proceedings of the Beyond Conventional Adaptive Optics (2001).
[19] A. Riccardi, N. Bindi, R. Ragazzoni, S. Esposito, P. Stefanini, SPIE Proc. 3353 (1998) 941.
[20] D. Fried, JOSA 55 (1965) 1427.
[21] S. Wadle, D. Wuest, J. Cantalupo, R.S. Lakes, Opt. Eng. 33 (1994) 213.
[22] M. Wenyon, P. Ralli, Society for Information and Display 94 Digest (1994) 285.
[23] S. Wadle, R.S. Lakes, Opt. Eng. 33 (1994) 1084.
[24] C. Gu, J.R. Lien, F. Dai, JOSAa 13 (1996) 1704.
[25] R. Ragazzoni, E. Diolaiti, E. Vernet, J. Farinato, unpublished.